High-Efficiency Leaky-Wave Antenna Array With Sidelobe Suppression and Multibeam Generation

Yunjie Geng, Junhong Wang, *Senior Member, IEEE*, Yujian Li, Zheng Li, Meie Chen, and Zhan Zhang

***Abstract*—A novel kind of high-efficient leaky-wave antenna array based on substrate integrated waveguide is investigated for sidelobe suppression and multibeam generation. The antenna array is designed upon a previous work with two feeding ports, and a tapered radiating slot array introduced. This kind of structure enables the array to have not only the compact architecture and high efficiency, but also the multibeam radiation and low sidelobe level (SLL). Different beams are generated by feeding the array from different input ports, and the SLL is reduced by the tapered slot lengths. The array was fabricated and measured, and the results are consistent with that of simulation.**

***Index Terms*—Antenna arrays, leaky-wave antennas (LWAs), low sidelobe, multibeam, substrate integrated waveguide (SIW).**

I. Introduction

LEAKY-WAVE antenna (LWA) is known for its featured advantages, such as high gain, simple feeding structure, and outstanding capability of frequency beam scanning [1]. Regardless of these advantages, this kind of antenna is usually classified as low-radiation-efficiency antenna because matching load must be used at the end to avoid the reflection. Several designs of LWAs with high efficiency have been presented in [2] and [3]. In our previous work [4], a new LWA array with a simple power-recycling feeding network was proposed and realized on the substrate integrated waveguide (SIW), which used the hybrid radiation of fundamental wave and –1th space harmonic of periodic structures. The proposed array showed a significant improvement of the radiation efficiency.

In this letter, the method of improving the radiation efficiency of LWA [4] is used to design a new LWA array, which can generate two different beams with low sidelobes when feeding from different input ports. Compared to the antenna array in [4], besides the compact structure and high radiation efficiency, the radiation beam of the new proposed array can be shifted in two different directions at a fixed frequency. Meanwhile, the sidelobe level (SLL) of this array is reduced by means of slot length tapering, which results in a Taylor distribution of aperture field [5].

Manuscript received June 30, 2017; revised August 4, 2017; accepted August 14, 2017. Date of publication August 29, 2017; date of current version October 16, 2017. This work was supported in part by the National Nature Science Foundation of China under Grant 61331002, and in part by the National Program on Key Basic Research Project under Grant 2013CB328903. *(Corresponding Author: Yunjie Geng.)*

The authors are with the Key Laboratory of All Optical Network and Advanced Telecommunication Network of Ministry of Education, Institute of Lightwave Technology, Beijing Jiaotong University, Beijing 100044, China (e-mail: 15111009@bjtu.edu.cn; wangjunh@bjtu.edu.cn; liyujian@bjtu.edu.cn; lizheng@bjtu.edu.cn; mechen@bjtu.edu.cn; zhangzhan@bjtu.edu.cn).

Color versions of one or more of the figures in this letter are available online at http://ieeexplore.ieee.org.

Digital Object Identifier 10.1109/LAWP.2017.2746090

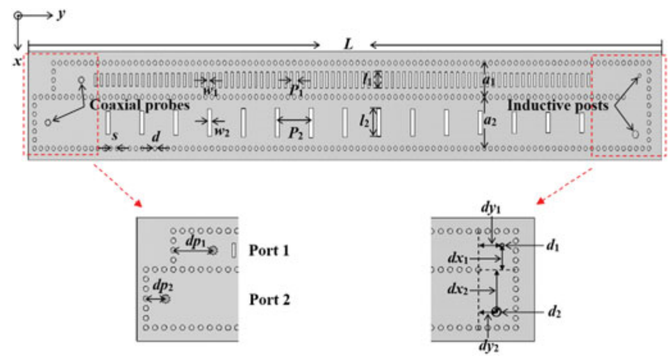

Fig. 1. Geometry of the proposed SIW antenna array. $L = 160$ mm, $d = 0.9$ mm, $s = 1.6$ mm, $a_1 = 6.4$ mm, $a_2 = 9.6$ mm, $w_1 = 0.5$ mm, $w_2 = 1$ mm, $P_1 = 1.5$ mm, $P_2 = 8.55$ mm, $dp_1 = 7$ mm, $dp_2 = 3.4$ mm, $d_1 = 0.74$ mm, $d_2 = 1.5$ mm, $dx_1 = 4$ mm, $dy_1 = 4$ mm, $dx_2 = 7$ mm, $dy_2 = 3$ mm.

The antenna design is described in detail in Section II. The prototype is shown in Section III, and the measured results are compared with the simulated results. Finally, conclusions are drawn in Section IV.

II. Antenna Design

Fig. 1 demonstrates the geometry of the proposed multibeam radiation and low-SLL LWA array, it contains two single LWAs with different periodic slots etched on the SIW. The slot lengths along the antennas are tapered. Two inductive posts at the end of structure and two coaxial probes at the beginning are designed for impedance matching and feeding. The structure of SIW is similar to that in [4] and the design rule is the same as that in [6].

As can be seen, there are two ports connected by two coaxial probes with 50 Ω; when one is used as the input port, the other is terminated with matching load. Two input ports correspond to two beam directions. SMA connectors are used to support the coaxial probes [5], [7]. The two inductive posts in the SIW bends play an important role in reducing reflection, and a desirable return loss can be obtained by optimizing their positions and diameters [8]. Compared with the previous antenna array in [4], this antenna array shows an asymmetric architecture that consists of two single LWAs with different periodic slots and different waveguide widths, working on fundamental ($m = 0$) wave radiation and –1th ($m = -1$) space harmonic radiation, respectively [9]. Due to the replacement of microstrip line feeding with the coaxial probe feeding, the size of this array is more compact than the previous one. More importantly, the two ports can both be the input ports; when feeding from different input ports, the antenna can radiate in forward and backward

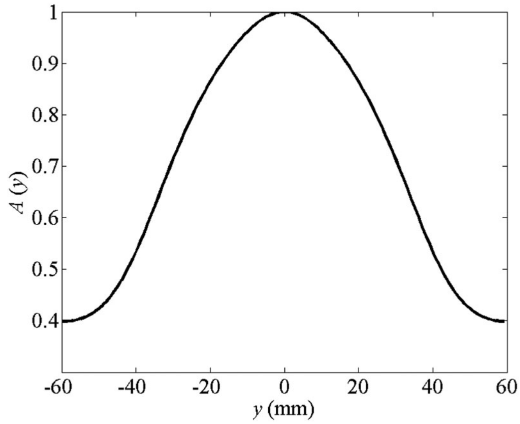

Fig. 2. Aperture distribution of field amplitude.

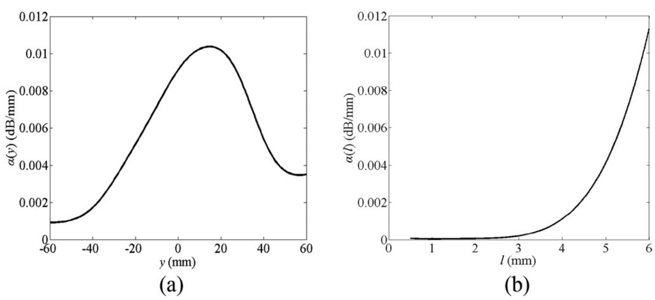

Fig. 3. (a) Leakage rate versus position y. (b) Leakage rate versus the slot length l_2.

directions, respectively; and the high efficiency property remains the same as we mentioned before.

The total length of the array is denoted by L. The substrate has a thickness of $h = 1.524$ mm and a dielectric constant of $\varepsilon_r = 3$. The widths of the two SIWs are a_1 and a_2, corresponding to the equivalent widths of rectangular waveguides $w_{\text{eff}1}$ and $w_{\text{eff}2}$, respectively. The length and width of the slots are l_n and w_n, and the period of the slots is P_n $(n = 1, 2)$. The value of P_1 is selected to ensure that the antenna radiates only from the fundamental wave, and the value of P_2 is selected to ensure that the antenna radiates only from –1th space harmonic [10]. The design procedure and basic parameters of the antennas are the same as those in [4], but the length of the slots is tapered for reducing the SLL.

Both of the LWAs are designed to have aperture distributions of field amplitude satisfying the Taylor distribution $A(y)$ with -25 dB SLL, as shown in Fig. 2 [11]. Thus, the leakage rate $\alpha(y)$ can be calculated from [1]

$$\alpha(y) = \frac{0.5 \times \left|A(y)^2\right|}{\frac{1}{\eta}\int_{-L/2}^{L/2}\left|A(\zeta)^2\right| d\zeta - \int_{-L/2}^{y}\left|A(\zeta)^2\right| d\zeta}. \quad (1)$$

In (1), η is the efficiency of antenna terminated with a load. Here, we take the –1th space harmonic radiation antenna $(n = 2)$ as an example to demonstrate the design process. Taking $\eta_2 = 0.6$, the leakage rate versus position can be computed by (1) and is shown in Fig. 3(a). As is well known, $\alpha(y)$ is physically determined by the slot length l_2. To figure out the relationship between them, a set of uniform transverse slotted antennas with different slot length l_2 is simulated with the other parameters remaining the same as the nonuniform antenna. The results are given in Fig. 3(b). Combining Fig. 3(a) and (b), the slot length $l_2(y)$ at different position is easily obtained, which is given in Fig. 4(a) [12]. Finally, the nonuniform periodic slots LWA is achieved. The design procedure for the fundamental wave radiation antenna $(n = 1)$ is the same, and the results of the slot length $l_1(y)$ are given in Fig. 4(b).

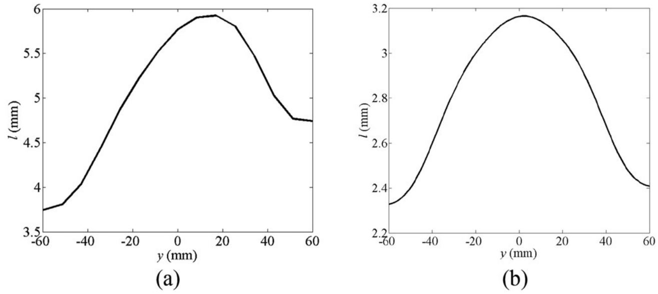

Fig. 4. Relationship between slot length and position. (a) l_2 versus y. (b) l_1 versus y.

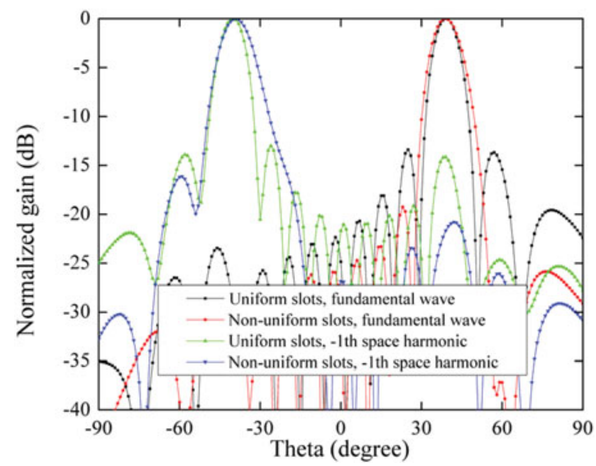

Fig. 5. Simulated normalized gain of two single antennas. Fundamental wave radiation LWA and -1th space harmonic radiation LWA.

III. Simulated and Measured Results

In order to see the reduction efficiency of sidelobes of the nonuniform-slot-length antennas, the two nonuniform-slot-length antennas are simulated individually first, and the radiation patterns (yz plane) are given in Fig. 5. For comparison, the results of two uniform slotted antennas with slot lengths of 3 and 5 mm are also given. The operating frequency is 16 GHz. It is obviously seen that by tuning the slot length in a tapered way, noticeable reduction in SLL can be found in both the nonuniform-slot-length antennas, which proves the effect of the tapering slot length design. In addition, the beams of these two antennas are opposite in the space, which means that when these two antennas are integrated into one array as shown in Fig. 1, the radiations from fundamental wave radiation antenna and -1th space harmonic radiation antenna can effectively superpose as we desired. However, it is also found that compared to that of the uniform-slots antenna, the beam angle of nonuniform-slots antenna has a slight drift due to the phase constant changing caused by the variation of slot length, as mentioned in [5], and the beamwidth is broadened a little bit, especially for the –1th

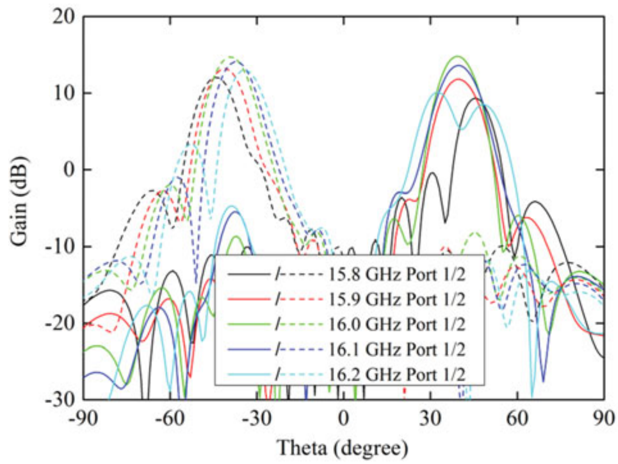

Fig. 6. Frequency characteristics of the antenna array in terms of the radiation pattern from different input ports.

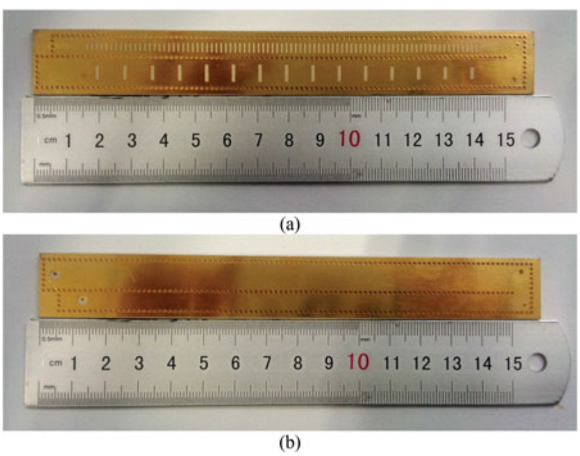

Fig. 7. Prototype of the proposed SIW antenna array as shown in Fig. 1. (a) Top view. (b) Back view.

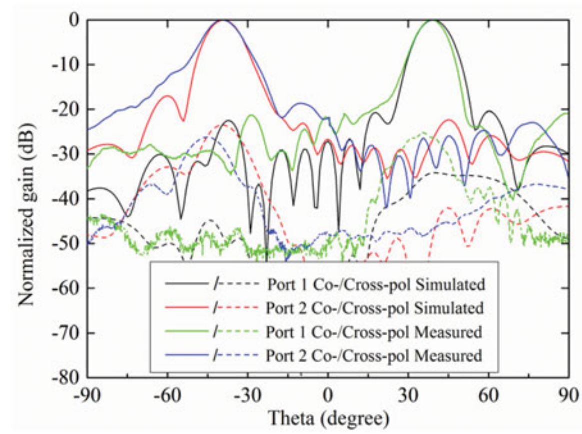

Fig. 8. Simulated and measured copolarization and cross-polarization patterns of the proposed antenna array at 16 GHz from different input ports.

space harmonic radiation antenna, but this has little influence on the performance of the proposed array.

As discussed in [4], the radiation beams of the LWAs working on fundamental radiation and the –1th spatial harmonic radiation will strictly point to the same direction only at the frequency we design, which means that the proposed antenna array can only work in a certain frequency. However, owing to the finite beamwidth of the radiation beams, the antenna array can work in a certain frequency band without splitting of the whole radiation beam. Fig. 6 gives the frequency characteristics of the antenna array from different input ports in terms of the radiation pattern. As we can see, with the frequency increasing or decreasing from 16 GHz, the performance of this array gets worse. The main beam will split into two lobes when the frequency increases or decreases by 200 MHz, which indicates that the frequency bandwidth of this array is about 400 MHz.

Fig. 7 shows the fabricated prototype of the proposed antenna array integrated by the above two nonuniform-slot-length LWAs. It has a compact size of $160 \times 20\,\mathrm{mm}^2$. The simulated and measured copolarization and cross-polarization patterns (*yz* plane) of the antenna array are depicted in Fig. 8. The cross-polarization level is less than -20 dB. As mentioned above, the array can radiate in both forward and backward directions when the signal is fed into different input ports. When the signal is fed into the fundamental wave radiation antenna from port 1, the array radiates in forward direction at about 39°. When the signal is fed into the –1th space harmonic radiation antenna from port 2, the array radiates in backward direction at about $-39°$. However, as we can see from Fig. 8, when the signal is fed into the array from port 2, both the simulation and measurement radiation patterns are not as good as those fed from port 1. Because in our design we take port 1 as the input port and port 2 is terminated with matching load, the lengths of the slots are not symmetrical along *y*-axis, as shown in Fig. 4. In this case, when we take port 2 as the input port, the aperture distributions of field amplitude, both for the fundamental wave radiation LWA and –1th space harmonic radiation LWA, will not satisfy the Taylor distribution. However, since the radiation efficiencies of these two antennas are not designed so high, the attenuation rate along the antennas is not too large, and the symmetry of the slot lengths is not distorted too much, therefore the difference between radiation patterns for feeding from ports 1 and 2 is not so significant, as depicted in Fig. 8. The measured radiation patterns are in good agreement with those of simulation. The slight shift of the left sidelobe when feeding from port 2, as observed in the measured pattern, is mainly caused by the measurement error in antenna alignment.

The simulated and measured *S*-parameters of the proposed array for different input ports are demonstrated in Fig. 9. It can be seen that S_{11} and S_{22} are lower than -10 dB in the working frequency band for both the simulated and measured results. However, there are some discrepancies between the simulated and measured S_{21} and S_{12}. On one hand, it is because of the manufacturing tolerance in the coaxial probe feeding structure and the error in the processing of measurement. On the other hand, because the simulated and measured S_{21} and S_{12} are both lower than -10 dB at the working frequency, which means most of the input power leaks out before reaching the termination, the absolute difference between the simulated and measured results is not so big for acceptance.

The simulated and measured radiation characteristics of the antenna array at 16 GHz are summarized in Table I. The radiation efficiencies from CST Microwave Studio simulation for input port 1 and port 2 are 85.9% and 84.4%, respectively, as shown in Table I. The simulated and measured total power ratio for dissipation and radiation ($\eta_{\text{total}} = 1 - S_{11}^2 - S_{21}^2$) is

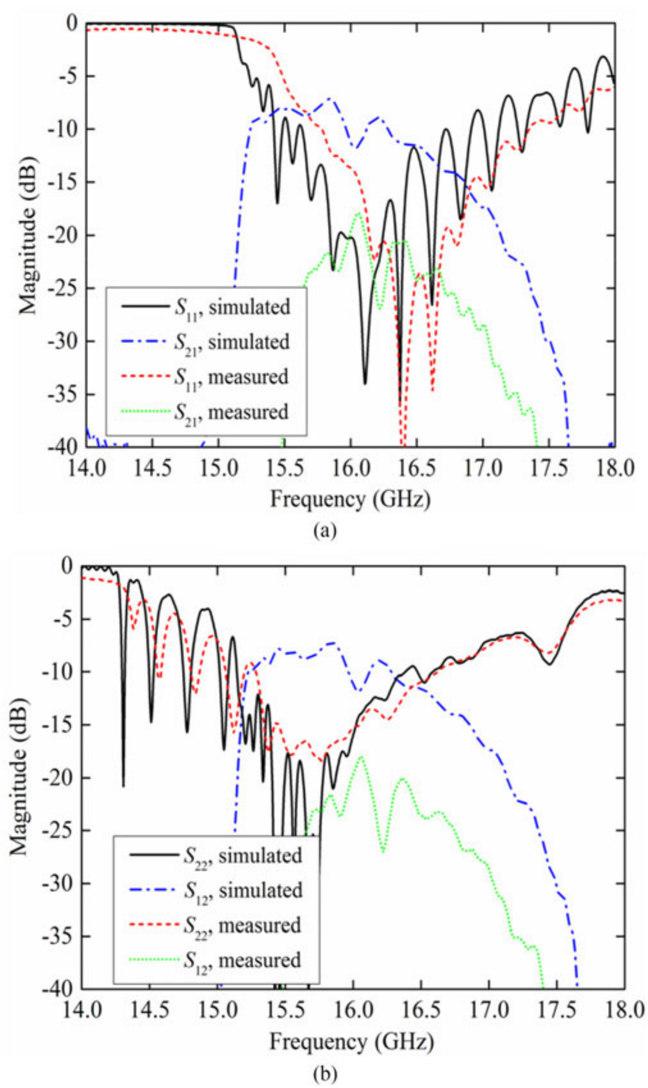

Fig. 9. Simulated and measured *S*-parameters of the proposed array. (a) Input from port 1. (b) Input from port 2.

TABLE I
RADIATION CHARACTERISTICS OF THE SIW LWA ARRAY

Input Port 1/2	Simulation	Measurement
SLL (dB)	–20.8/–16.7	–20.8/–18.7
Gain (dB)	14.85/14.79	13.62/13.57
Radiation efficiency	85.9%/84.4%	n. a.
Total power ratio for dissipation and radiation ($\eta_{\text{total}} = 1 - S_{11}^2 - S_{21}^2$)	91.5%/89.8%	99.8%/99.9%

also given for comparison. As we can see, the measured total power ratio for dissipation and radiation is higher than the simulation one. This is mainly due to the probe feeding connectors used in the experiment, which cause additional loss. A comparison considering the SLL, antenna size, bandwidth, and radiation efficiency between this work and the references is given in Table II, which shows the obvious superiority of this proposed design in compact size, high efficiency, and the generation of multibeam radiation due to the novel structure.

TABLE II
COMPARISON BETWEEN PROPOSED AND REPROPOSED LOW-SIDELOBE SIW LWAS

Ref.	SLL (dB)	Antenna Size(mm^2)	Bandwidth (%)	Radiation Efficiency(%)
[5]	Below -20	$14.2\lambda_0 \times 1.6\lambda_0$	14.1	75
[12]	-28.7	$3.6\lambda_0 \times 1.6\lambda_0$	31.7	n. a.
This work (port 1/2)	$-20.8/-16.7$	$8.5\lambda_0 \times 1.1\lambda_0$	9.4/12.5	85.9/84.4

IV. CONCLUSION

A low-SLL LWA array with high efficiency and multibeam generation is proposed and realized by SIW. The antenna array achieves a low SLL of -20.8 dB at 16 GHz by tuning slot length, and at least 84% power is radiated for both cases of feeding from the two ports. The design offers a more compact structure than the previously proposed antenna array. In addition, it can radiate in both forward and backward directions when fed from different input ports at a fixed frequency. The array can be extended to new arrays that can provide more input ports and realize multibeam radiation by integrating more periodic slot structures together.

REFERENCES

[1] A. Oliner and D. R. Jackson, "Leaky-wave antennas," in *Antenna Engineering Handbook*, J. L. Volakis, Ed. New York, NY, USA: McGraw-Hill, 2007.

[2] H. V. Nguyen, A. Parsa, and C. Caloz, "Power-recycling feedback system for maximization of leaky-wave antennas radiation efficiency," *IEEE Trans. Microw. Theory Techn.*, vol. 58, no. 7, pp. 1641–1650, Jul. 2010.

[3] H. V. Nguyen, S. Abielmona, and C. Caloz, "Highly efficient leaky-wave antenna array using a power-recycling series feeding network," *IEEE Antenna Wireless Propag. Lett.*, vol. 8, pp. 441–444, 2009.

[4] Y. Geng, J. Wang, Y. Li, Z. Li, M. Chen, and Z. Zhang, "Leaky-wave antenna array with a power-recycling feeding network for radiation efficiency improvement," *IEEE Trans. Antennas Propag.*, vol. 65, no. 5, pp. 2689–2694, May 2017.

[5] J. Liu, D. R. Jackson, Y. Li, C. Zhang, and Y. Long, "Investigations of SIW leaky-wave antenna for endfire-radiation with narrow beam and sidelobe suppression," *IEEE Trans. Antennas Propag.*, vol. 62, no. 9, pp. 4489–4497, Sep. 2014.

[6] F. Xu and K. Wu, "Guided-wave and leakage characteristics of substrate integrated waveguide," *IEEE Trans. Microw. Theory Techn.*, vol. 53, no. 1, pp. 66–73, Jan. 2005.

[7] S. Mukherjee, P. Chongder, K. V. Srivastava, and A. Biswas, "Design of a broadband coaxial to substrate integrated waveguide (SIW) transition," in *Proc. 2013 Asia-Pacific Conf. Microw.*, Seoul, South Korea, 2013, pp. 896–898.

[8] Z. C. Hao, W. Hong, H. Li, H. Zhang, and K. Wu, "Multiway broadband substrate integrated waveguide (SIW) power divider," in *Proc. Int. Symp. IEEE Antennas Propag. Soc.*, 2005, pp. 639–642, vol. 1A.

[9] J. Liu, D. R. Jackson, and Y. Long, "Substrate integrated waveguide (SIW) leaky-wave antenna with transverse slots," *IEEE Trans. Antennas Propag.*, vol. 60, no. 1, pp. 20–29, Jan. 2012.

[10] J. Wang, Y. Geng, C. Zhang, and X. Huo, "Radiation characteristic of the periodic leaky wave structure and its application to leaky wave antenna design," in *Proc. 2015 Asia-Pacific Microw. Conf.*, Nanjing, China, 2015, p. 1.

[11] T. T. Taylor, "Design of line-source antennas for narrow beamwidth and low side lobes," in *Trans. IRE Prof. Group Antennas Propag.*, vol. 3, no. 1, pp. 16–28, Jan. 1955.

[12] J. Wang, Y. Geng, and J. Wang, "Low-sidelobe non-uniform transverse slotted antenna array fed by substrate integrated waveguide," in *Proc. 2016 Int. Conf. IEEE Microw. Millimeter Wave Technol.*, Beijing, China, 2016, pp. 817–818.